

## LY $\alpha$ -EMITTING GALAXIES AT Z = 3.1: L\* PROGENITORS EXPERIENCING RAPID STAR FORMATION<sup>14</sup>

ERIC GAWISER<sup>1,2,3,4</sup>, HAROLD FRANCKE<sup>1,3</sup>, KAMSON LAI<sup>5</sup>, KEVIN SCHAWINSKI<sup>6</sup>, CARYL GRONWALL<sup>7</sup>, ROBIN CIARDULLO<sup>7</sup>, RYAN QUADRI<sup>1</sup>, ALVARO ORSI<sup>8</sup>, L. FELIPE BARRIENTOS<sup>8</sup>, GUILLERMO A. BLANC<sup>3,9</sup>, GIOVANNI FAZIO<sup>5</sup>, JOHN J. FELDMEIER<sup>10</sup>, JIA-SHENG HUANG<sup>5</sup>, LEOPOLDO INFANTE<sup>8</sup>, PAULINA LIRA<sup>3</sup>, NELSON PADILLA<sup>8</sup>, EDWARD N. TAYLOR<sup>11</sup>, EZEQUIEL TREISTER<sup>1,3,12</sup>, C. MEGAN URRY<sup>1,2,13</sup>, PIETER G. VAN DOKKUM<sup>1,2</sup>, SHANIL N. VIRANI<sup>1,2</sup>

### ABSTRACT

We studied the clustering properties and multiwavelength spectral energy distributions of a complete sample of 162 Ly $\alpha$ -emitting (LAE) galaxies at  $z \simeq 3.1$  discovered in deep narrow-band MUSYC imaging of the Extended Chandra Deep Field South. LAEs were selected to have observed frame equivalent widths  $> 80 \text{ \AA}$  and emission line fluxes  $> 1.5 \times 10^{-17} \text{ ergs cm}^{-2} \text{ s}^{-1}$ . Only 1% of our LAE sample appears to host AGN. The LAEs exhibit a moderate spatial correlation length of  $r_0 = 3.6_{-1.0}^{+0.8} \text{ Mpc}$ , corresponding to a bias factor  $b = 1.7_{-0.4}^{+0.3}$ , which implies median dark matter halo masses of  $\log_{10} M_{\text{med}} = 10.9_{-0.9}^{+0.5} M_{\odot}$ . Comparing the number density of LAEs,  $1.5 \pm 0.3 \times 10^{-3} \text{ Mpc}^{-3}$ , with the number density of these halos finds a mean halo occupation  $\sim 1$ –10%. The evolution of galaxy bias with redshift implies that most  $z = 3.1$  LAEs evolve into present-day galaxies with  $L < 2.5L^*$ , whereas other  $z > 3$  galaxy populations typically evolve into more massive galaxies. Halo merger trees show that  $z = 0$  descendants occupy halos with a wide range of masses, with a median descendant mass close to that of  $L^*$ . Only 30% of LAEs have sufficient stellar mass ( $> \sim 3 \times 10^9 M_{\odot}$ ) to yield detections in deep Spitzer-IRAC imaging. A two-population SED fit to the stacked  $UBVRIzJK+[3.6,4.5,5.6,8.0] \mu\text{m}$  fluxes of the IRAC-undetected objects finds that the typical LAE has low stellar mass ( $1.0_{-0.4}^{+0.6} \times 10^9 M_{\odot}$ ), moderate star formation rate ( $2 \pm 1 M_{\odot} \text{ yr}^{-1}$ ), a young component age of  $20_{-10}^{+30} \text{ Myr}$ , and little dust ( $A_V < 0.2$ ). The best fit model has 20% of the mass in the young stellar component, but models without evolved stars are also allowed.

*Subject headings:* galaxies:high-redshift - galaxies:formation - galaxies:evolution - large-scale structure of universe

### 1. INTRODUCTION

The discovery of high-redshift Ly $\alpha$ -emitting galaxies (LAEs) opened a new frontier in astronomy (Cowie & Hu 1998; Hu et al. 1998). Because the Ly $\alpha$  line is easily quenched, a galaxy with detectable Ly $\alpha$  emission is likely dust-free, i.e., in the initial phases of a burst of star formation.

Electronic address: gawiser@physics.rutgers.edu

<sup>1</sup> Department of Astronomy, Yale University, New Haven, CT.

<sup>2</sup> Yale Center for Astronomy & Astrophysics, Yale University, New Haven, CT.

<sup>3</sup> Departamento de Astronomía, Universidad de Chile, Casilla 36-D, Santiago, Chile.

<sup>4</sup> Department of Physics and Astronomy, Rutgers University, Piscataway, NJ.

<sup>5</sup> Harvard-Smithsonian Center for Astrophysics, Cambridge, MA.

<sup>6</sup> University of Oxford, Astrophysics, Keble Road, Oxford UK.

<sup>7</sup> Department of Astronomy and Astrophysics, Pennsylvania State University, University Park, PA.

<sup>8</sup> Departamento de Astronomía y Astrofísica, Pontificia Universidad Católica de Chile, Santiago, Chile.

<sup>9</sup> Department of Astronomy, University of Texas at Austin, Austin, TX.

<sup>10</sup> Department of Physics & Astronomy, Youngstown State University, Youngstown, OH.

<sup>11</sup> Leiden Observatory, Leiden, Netherlands.

<sup>12</sup> European Southern Observatory, Santiago, Chile.

<sup>13</sup> Department of Physics, Yale University, New Haven, CT.

<sup>14</sup> This work is based on archival data obtained with the Spitzer Space Telescope, which is operated by the Jet Propulsion Laboratory, California Institute of Technology under a contract with NASA, with the 6.5 m Magellan-Baade telescope, a collaboration between the Observatories of the Carnegie Institution of Washington, University of Arizona, Harvard University, University of Michigan, and Massachusetts Institute of Technology, and at Cerro Tololo Inter-American Observatory, a division of the National Optical Astronomy Observatories, which is operated by the Association of Universities for Research in Astronomy, Inc. under cooperative agreement with the National Science Foundation.

The Ly $\alpha$  lines have large equivalent widths ( $20 \text{ \AA} < EW_{\text{rest}} < \sim 100 \text{ \AA}$ ) and broad velocity widths ( $100 \text{ km s}^{-1} < \text{FWHM} < 800 \text{ km s}^{-1}$ ) and are often asymmetric, indicative of high-redshift galaxies undergoing active star-formation (e.g., Manning et al. 2000; Kudritzki et al. 2000; Arnaboldi et al. 2002; Rhoads et al. 2003; Dawson et al. 2004; Hu et al. 2004; Venemans et al. 2005; Matsuda et al. 2006; Gronwall et al. 2007).

Other high-redshift galaxy populations (including Lyman break galaxies, Distant Red Galaxies, Sub-Millimeter Galaxies) exhibit strong clustering and should evolve into elliptical and giant elliptical galaxies today (Adelberger et al. 2005b; Quadri et al. 2007; Webb et al. 2003). These objects were selected by unusually strong rest-frame continuum emission in the ultraviolet, optical, and far-IR respectively, resulting in  $10^{10} L_{\odot} \leq L_{\text{bol}} \leq 10^{12} L_{\odot}$  (Reddy et al. 2006). Such strong continua appear to occur primarily in deep potential wells that are strongly biased versus the general distribution of dark matter halos. LAEs instead offer the chance to probe the faint end of the (bolometric) luminosity function of high-redshift galaxies, which contains the majority of galaxies. The strong Ly $\alpha$  emission line allows detection and spectroscopic confirmation of LAEs with typical bolometric luminosities  $\simeq 10^{10} L_{\odot}$ . A detailed calculation of the LAE luminosity function at  $z \simeq 3.1$  is given in Gronwall et al. (2007).

Spectral energy distribution (SED) modelling of the stacked  $UBVRIzJK$  photometry of 18 LAEs in the Extended Chandra Deep Field-South (ECDF-S) (Gawiser et al. 2006a) showed the average galaxy to have low stellar mass ( $< 10^9 M_{\odot}$ ) and minimal dust (see also Nilsson et al. 2007). LAEs have the highest *specific* star formation rates (defined as SFR divided by stellar mass) of any type of galaxy, implying the youngest

ages (Castro Cerón et al. 2006). Because  $\text{Ly}\alpha$  emission is easily quenched by dust, LAEs have often been characterized as protogalaxies experiencing their first burst of star formation (e.g. Hu & McMahon 1996). However, the differing behavior of  $\text{Ly}\alpha$  and continuum photons encountering dust and neutral gas makes it possible for older galaxies to exhibit strong  $\text{Ly}\alpha$  emission when morphology and kinematics favor the escape of these photons towards Earth (Neufeld 1991; Haiman & Spaans 1999; Hansen & Oh 2006). This could allow older, dusty galaxies with actively star-forming regions to exhibit  $\text{Ly}\alpha$  emission with high equivalent width.

SED modelling of LAEs using Spitzer-IRAC (Fazio et al. 2004) to probe rest-frame near-infrared wavelengths, where old stars dominate the emission, has yielded mixed results. Pirzkal et al. (2007) report extremely young ages of a few Myr and low stellar masses ( $10^6 M_\odot < M_* < 10^8 M_\odot$ ) from SED modelling of 9 LAEs at  $4.0 < z < 5.7$  in the Hubble Ultra Deep Field. However, Lai et al. (2007a) performed SED fitting to 3 LAEs with IRAC detections out of a sample of 12  $z = 5.7$  LAEs in GOODS-N and found ages as high as 700 Myr and significant stellar masses ( $10^9 < M_\odot < 10^{10}$ ), making it appear that these LAEs were not undergoing their first burst of star formation. The 9/12 LAEs lacking IRAC detections are presumably younger and less massive and might lack an evolved population. Investigating the nature of the LAEs without IRAC detections requires a stacking approach to see if the typical LAE stellar mass is low enough to have been generated in a single ongoing starburst. Stacking will yield the best results when applied to a large statistical sample of LAEs in a region with deep IRAC imaging.

Gronwall et al. (2007) present the largest available sample of LAEs in an unbiased field, 162 LAEs at  $z = 3.1$  in the ECDF-S discovered as part of the MUSYC survey (Gawiser et al. 2006b, <http://www.astro.yale.edu/MUSYC>). The ECDF-S has been targeted with deep narrow-band imaging and multi-object spectroscopy, complemented by public broadband  $UBVRIZJK$ , Spitzer+IRAC and Chandra+ACIS-I imaging. We improve the constraints of Gawiser et al. (2006a) using the MUSYC  $UBVRIZJK$  photometry of our larger sample of LAEs and adding IRAC [ $3.6\mu\text{m}, 4.5\mu\text{m}, 5.8\mu\text{m}, 8.0\mu\text{m}$ ] Cycle 2 legacy images from SIMPLE (Spitzer IRAC/MUSYC Public Legacy of the ECDF-S, <http://www.astro.yale.edu/dokkum/simple>).

This Letter summarizes our imaging and spectroscopic observations of LAEs, presents our results from clustering analysis and SED modelling, and discusses the implications for the formation process of typical present-day galaxies. We assume a  $\Lambda$ CDM cosmology consistent with WMAP results (Spergel et al. 2007) with  $\Omega_m = 0.3, \Omega_\Lambda = 0.7, H_0 = 70 \text{ km s}^{-1} \text{ Mpc}^{-1}$ , and rms dark matter fluctuations on  $8h^{-1} \text{ Mpc}$  scales given by  $\sigma_8 = 0.9$ . All correlation lengths and number densities are comoving. We have suppressed factors of  $h_{70}$  in reporting correlation lengths, number densities, dark matter masses, stellar masses and star formation rates.

## 2. OBSERVATIONS

Our narrow-band  $4990\text{\AA}$  and  $UBVRIZJK$  images of ECDF-S are described in Gronwall et al. (2007) and Gawiser et al. (2006a) and are available at <http://www.astro.yale.edu/MUSYC>. The final images cover  $31.5' \times 31.5' = 992 \text{ arcmin}^2$  to a narrow-band completeness limit of  $\sim 1.5 \times 10^{-17} \text{ ergs cm}^{-2} \text{ s}^{-1}$  ( $\text{AB}=25.4$

in the  $50\text{\AA}$  FWHM NB4990 $\text{\AA}$  filter). Figure 1 shows our complete sample of 162 strong  $\text{Ly}\alpha$  emitting galaxies at  $z \simeq 3.1$  with equivalent width  $> 80\text{\AA}$  in the observed frame. 28 LAEs lie in the region surveyed by the GOODS Legacy program (Dickinson et al. 2003).

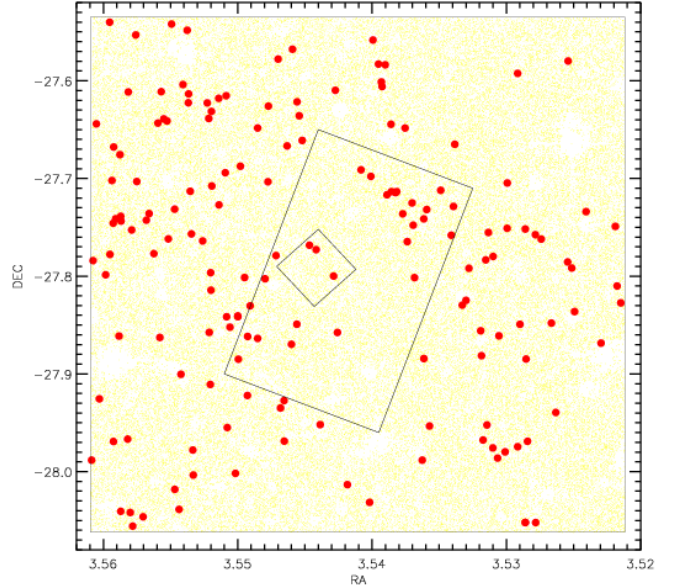


FIG. 1.— Plot of the  $31.5' \times 31.5'$  Extended Chandra Deep Field-South, showing the MUSYC BVR-selected catalog of 84490 objects as tiny dots. The rectangle shows the GOODS-S region, and the inner square shows the Hubble Ultra Deep Field.  $\text{Ly}\alpha$ -emitting galaxies at  $z = 3.1$  are shown as solid circles.

Multi-object spectroscopy of 92 LAE candidates, along with other MUSYC targets, was performed with Magellan-Baade+IMACS on Oct. 26-27, 2003, Oct. 7-8, 2004, Feb. 4-7, 2005, Nov. 2-3, 2005, Oct. 25-27, 2006, Nov. 21-22, 2006 and Feb. 18-20, 2007. The 300 line/mm grism was used with  $1.2''$  slitlets to cover  $4000 - 9000\text{\AA}$  at a resolution of  $R = 640$  i.e.,  $470 \text{ km s}^{-1}$ , at the wavelength of  $\text{Ly}\alpha$  emission. Mask exposure times ranged from 2 to 5 hours, with the longer exposures sufficient to detect  $\text{Ly}\alpha$  emission lines down to our completeness limit of  $\sim 1.5 \times 10^{-17} \text{ ergs cm}^{-2} \text{ s}^{-1}$ , assuming clear conditions and minimal slit losses. Details of our spectroscopy will be given in P. Lira et al. (in prep). Redshifts were confirmed to lie at  $3.08 < z < 3.14$  for 61 of the LAEs, with 1 interloping AGN at  $z = 1.60$  where  $[\text{C III}]\lambda 1909$  falls in the narrowband filter, and the other 30 objects lacking sufficient S/N to yield redshifts. Our success rate for the slit-masks with the highest S/N was 90%, setting an upper limit of 10% on possible contamination of our LAE sample. The rate of non-detections was higher in masks with shorter exposure times resulting from weather or instrument challenges, consistent with the reduced S/N. Our spectroscopy shows that the sample is not contaminated by  $z = 0.34$   $[\text{O II}]$  emission-line galaxies, which are the typical interlopers for narrowband-selected LAE samples. These have been eliminated by requiring observer's-frame  $\text{EW} > 80\text{\AA}$  which eliminates all but the rarest  $[\text{O II}]$  emitters (Terlevich et al. 1991, Hogg et al. 1998, Stern et al. 2000).

The  $\text{Ly}\alpha$  emission in LAEs appears to derive from star formation rather than AGN activity; only 2/162 objects in our

complete sample are detected as X-ray sources in the Chandra catalogs of CDF-S and ECDF-S (Alexander et al. 2003; Lehmer et al. 2005; Virani et al. 2006). One is the  $z = 1.6$  interloper but the other is at  $z = 3.092$ . One additional object at  $z = 3.117$  is detected in X-ray photometry at the narrow-band source position. At  $z = 3.1$ , Chandra receives X-ray emission from 2–30 keV (rest-frame), meaning that Compton thick obscuration ( $N_{\text{H}} > \sim 10^{23} \text{cm}^{-2}$ ) is needed to hide AGN. Even such heavily obscured AGN are likely to reveal their presence via narrow emission lines, which should be indicated by high-ionization UV lines like C IV accompanying Ly  $\alpha$ . Amongst our LAE spectra, only the three X-ray sources show signs of AGN activity in the form of emission lines other than Ly  $\alpha$ , and the other 159 LAEs are undetected in a stacked X-ray image (Gronwall et al. 2007). We therefore expect that very few LAEs contain AGN that dominate their Ly $\alpha$  or continuum emission. Our two X-ray sources at  $z = 3.1$  imply that AGN are present in only  $1.2 \pm 0.9\%$  of Ly  $\alpha$  selected galaxies at this redshift. We restrict our subsequent analysis to the 159 LAEs without X-ray detections.

3. CLUSTERING ANALYSIS

We used the Landy & Szalay (1993) estimator to measure the angular correlation function using histograms of pairs of points at separation  $\theta$  between the data catalog ( $D$ ) and itself ( $DD$ ) as well as the cross-correlation and autocorrelation with a set of random catalogs ( $R$ ). We modelled this observed correlation function as an intrinsic  $w(\theta)$  minus the “integral constraint” caused by estimating the sky density of LAEs from our own survey (see Peebles 1980; Infante 1994, H. Francke et al. in prep)

$$\frac{DD(\theta) - 2DR(\theta) + RR(\theta)}{RR(\theta)} = w(\theta) - \sigma^2(1 + w(\theta)) \quad , \quad (1)$$

$$\text{where } \sigma^2 = \frac{1}{\Omega^2} \iint_{\Omega} w(\theta_{12}) d\Omega_1 d\Omega_2 \quad . \quad (2)$$

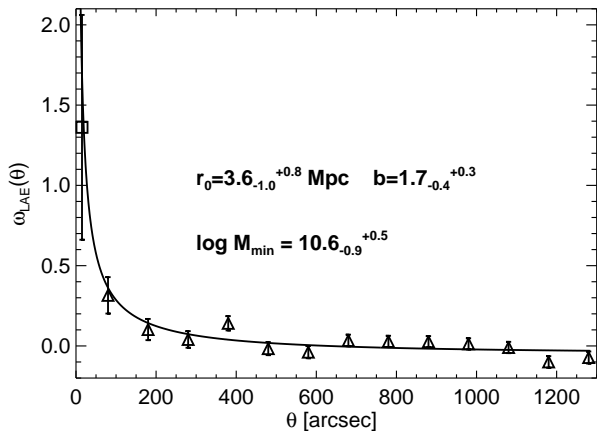


FIG. 2.— Angular auto-correlation function data with best-fit model (solid line) and best-fit spatial correlation length and dark matter halo bias and mass parameters listed. The bin below 30'' (square) is not used in the fit.

Figure 2 shows our binned data along with the best-fit model. Error bars show the uncertainties in each bin of  $\sigma_w(\theta) = (1 + w(\theta)) / \sqrt{RR(\theta)}$  (Landy & Szalay 1993; Gawiser et al. 2006b). The analysis was restricted to scales

larger than 30'' ( $\approx 1$  comoving Mpc) that are insensitive to the possible presence of multiple LAEs in some dark matter halos. In order to determine the expected redshift distribution,  $N_{exp}(z)$ , we performed a Monte Carlo simulation placing a large number of LAEs over the redshift range  $3 < z < 3.2$  and assigning them equivalent widths drawn at random from the equivalent width distribution observed for our sample (Gronwall et al. 2007). We then used the NB4990 filter bandpass to calculate the excess narrow-band flux that would be observed, removed all LAEs with “observed” equivalent width  $< 80 \text{\AA}$ , and measured the redshift distribution of the selected objects. Fig. 3 shows that the expected redshift distribution is narrower than the transmission curve. This occurs because LAEs far from the central redshift must have very high equivalent widths to be selected through narrowband excess, due to the reduced filter transmission at the wavelength of their Ly  $\alpha$  emission lines. Fig. 3 shows that the histogram of observed LAE redshifts is consistent with  $N_{exp}(z)$ . The only bin inconsistent with poisson fluctuations of the expected redshift distribution at the 9is is at  $3.085 \leq z < 3.090$ , which displays a  $3\sigma$  excess, revealing an overdensity at this redshift.

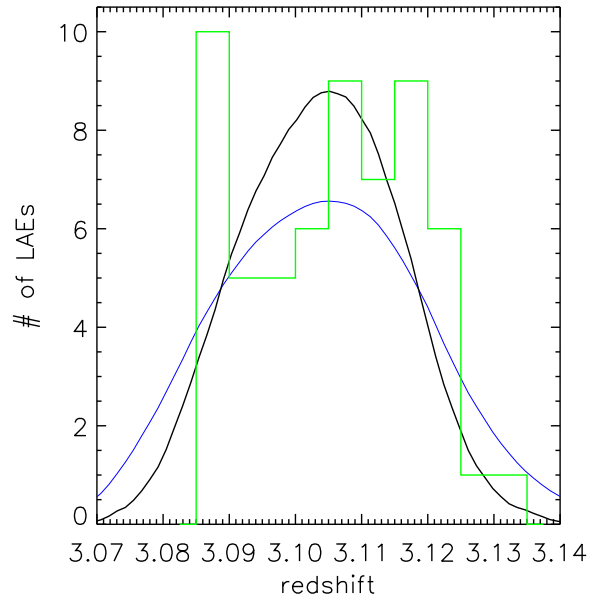


FIG. 3.— Histogram of LAE redshifts in ECDF-S. The thin solid curve is the filter transmission curve normalized to have the same area, and the thick solid curve is the expected redshift distribution described in the text.

We used  $N_{exp}(z)$  to deproject the angular correlation function, following Simon (2007). In order to avoid degeneracy between the clustering length  $r_0$  and the power-law index  $\gamma$  in the underlying spatial correlation function,  $\xi(r) = (r/r_0)^{-\gamma}$ , we assumed a typical power-law with  $\gamma = 1.8$ . This yielded a moderate clustering length,  $r_0 = 3.6_{-1.0}^{+0.8}$  Mpc (comoving). The narrow redshift distribution of narrow-band selected LAEs reduces the loss of angular clustering signal due to projection, allowing a high S/N measurement of moderate clustering. Following Quadri et al. (2007), this value of  $r_0$  corresponds to stronger clustering than the dark matter at  $z = 3.1$  by a bias factor  $b = 1.7_{-0.4}^{+0.3}$ . Note that bias factors are robust to the degeneracy between  $r_0$  and  $\gamma$ . This bias factor is shared by the population of dark matter halos with masses greater than

$\log_{10} M_{\text{min}} 10.6^{+0.5}_{-0.9} M_{\odot}$  (Sheth & Tormen 1999), implying a median dark matter halo mass of  $\log_{10} M_{\text{med}} = 10.9^{+0.5}_{-0.9} M_{\odot}$ . If 10% of the LAEs were unclustered low-redshift contaminants, the corrected value of  $r_0$  would be 10% higher, yielding halo masses  $\sim 50\%$  higher.

The comoving number density of our LAE sample is  $1.5 \pm 0.3 \times 10^{-3} \text{Mpc}^{-3}$  (Gronwall et al. 2007), where the uncertainty includes variance due to large-scale structure in our survey volume for objects with  $b = 1.7$  (Somerville et al. 2004). The number density of the corresponding dark matter halos is  $3^{+25}_{-2} \times 10^{-2} \text{Mpc}^{-3}$ , implying a “mean halo occupation” of  $5^{+10}_{-4.5}\%$  for the LAEs. There is significant freedom in how the LAEs could be assigned to this subset of the available dark matter halos. However, the LAE median halo mass must roughly follow the result  $\log_{10} M_{\text{med}} = 10.9^{+0.5}_{-0.9} M_{\odot}$  in order to explain the observed clustering bias.<sup>15</sup> Explorations of complex halo occupation distribution (HOD) models show that the assumption of one galaxy per halo made in our determination of  $M_{\text{med}}$  can cause additional uncertainties of up to 0.2dex at  $z = 3.1, b = 1.7$  (Lee et al. 2006; Zheng et al. 2007).

#### 4. SED MODELLING

Lai et al. (2007b) offer a detailed description of our IRAC photometry along with single-component SED fitting of the detected and undetected objects and a comparison of their continuum properties with those of Lyman break galaxies. 76 of our LAEs fall within regions of the SIMPLE images (which include the GOODS IRAC images) where the lack of bright neighbors enables IRAC photometry accurate to very low fluxes. Only 24 LAEs (30%) are detected by IRAC at fluxes above the  $2\sigma$  SIMPLE flux limit; these objects represent the high-mass end of the LAE mass function and appear to have stellar masses  $> 3 \times 10^9 M_{\odot}$ . Only 2 of these LAEs are detected in our  $J, K$  images, which are two magnitudes shallower than the IRAC 3.6, 4.5  $\mu\text{m}$  images. The IRAC-detected LAEs are brighter in the rest-UV and rest-optical continua, with mean R-band and 3.6  $\mu\text{m}$  fluxes corresponding to magnitude 25.4 and 24.4 respectively, compared with 26.7 and 26.6 for LAEs not detected by IRAC. In order to investigate the full SED of typical LAEs, which are too dim to be detected individually in our NIR and Spitzer images, we measured average fluxes from stacked images of the 52 LAEs (70%) lacking IRAC detections. We show the resulting SED in Fig. 4, where the  $V$ -band flux has been corrected for the contribution of the Ly $\alpha$  emission lines to this filter. Uncertainties in the stacked photometry were determined using bootstrap resampling to account for both sample variance and photometric errors.

Instead of modelling LAEs with a single stellar population, we analyzed the extent to which the data allow the presence of an underlying evolved population. We adapted the method of K. Schawinski et al. (in prep.) to model the star formation histories using a two-burst scenario with the old component as an instantaneous burst and the young component as an exponentially declining starburst with variable e-folding time. Maraston (2005) population synthesis models were used with metallicity ranging from 0.02 solar to solar, a Salpeter (1955) initial mass function, and the Calzetti et al. (2000) dust law. The best-fit model shown in Fig. 4 corresponds

<sup>15</sup> The quantity that must be preserved is the mean halo bias. The median halo mass is a simpler statistic that is also robust in typical HOD models, and the difference is far smaller than the reported uncertainties.

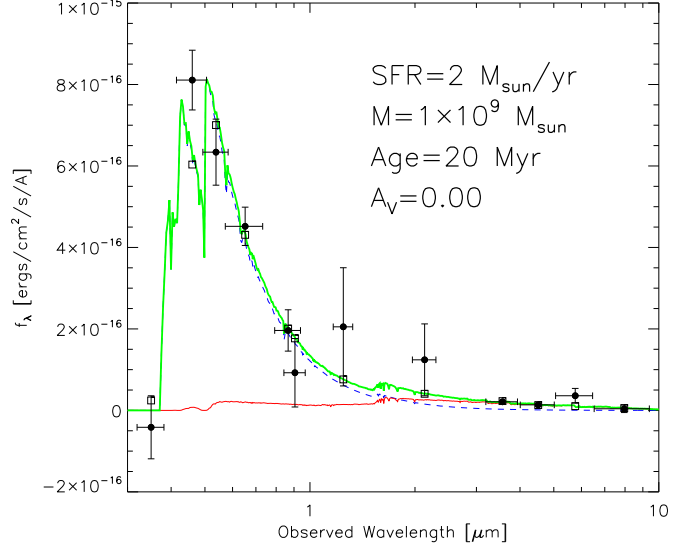


FIG. 4.— Datapoints show stacked flux densities ( $f_{\lambda}$ ) of LAEs lacking individual detections in the SIMPLE IRAC images, with  $1\sigma$  error bars. The thick solid curve gives the best-fit model described in the text, which is a sum of a young component (dashed curve) and an old component (thin solid curve). Squares show fluxes predicted by the best-fit model, which has  $\chi^2/\text{d.o.f.} = 14.6/12$ .

to a stellar mass of  $1.0^{+0.6}_{-0.4} \times 10^9 M_{\odot}$ , star formation rate of  $2 \pm 1 M_{\odot} \text{yr}^{-1}$ , and dust extinction  $A_V = 0.0^{+0.1}_{-0.0}$  (only positive values of  $A_V$  were considered). Figure 5 shows the results for the age of the young population versus the mass fraction of the young population. The young population has an age of  $20^{+30}_{-10} \text{Myr}$  with an e-folding timescale  $\tau = 750 \pm 250 \text{Myr}$  i.e., a nearly constant star formation rate. Although we did not include our narrow-band photometry in the SED analysis, the median LAE rest-frame equivalent width of 60  $\text{\AA}$  found by Gronwall et al. (2007) is consistent with that expected for normal stellar populations in this age range (Finkelstein et al. 2007). The age of the old population is not well constrained but has a best fit of 2 Gyr (the age of the universe at  $z = 3.1$ ).

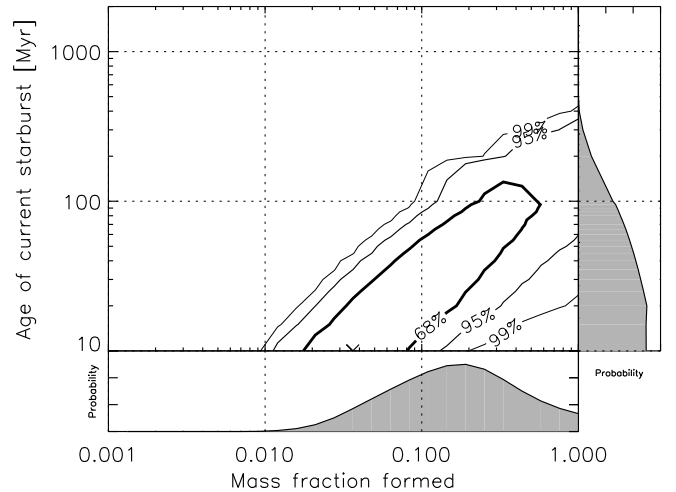


FIG. 5.— Constraints on age of the young stellar population versus its mass fraction.

The mass fraction formed in the current starburst is not

well constrained, and models where all of the stellar mass was produced in a current burst of star formation of age 60 to 350 Myr are allowed. Indeed, Lai et al. (2007b) performed a one-component SED fit with Maraston (2005) models and found a best-fit age of 100 Myr,  $\tau=250$  Myr,  $E(B-V)=0$ , and  $M_* = 3 \times 10^8 M_\odot$ . Our two-component best-fit is preferred to this, even accounting for the two extra degrees of freedom, but a single “ $\tau$ -model” population is not ruled out at 95% confidence (see Fig. 5).

5. DISCUSSION

In CDM cosmology, galaxy formation is an ongoing process caused by merging of lower-mass dark matter halos, which may already possess stars. Finding stellar population ages of  $< 100$  Myr is interesting. Our analysis of halo merger trees from the Milli-Millennium simulation (Springel et al. 2005) found the median age of dark matter halos with  $M > 10^{10.6} M_\odot$  at  $z = 3.1$  (defined as the age since half of the dark matter mass was accumulated) to be  $\sim 600$  Myr, with only  $< 10\%$  of halos younger than 100 Myr. If repeated LAE phases occur, the mean halo occupation of  $\sim 1\text{--}10\%$  can be interpreted as a “duty cycle” telling us what fraction of each halo’s lifetime is spent in the early phases of starbursts before significant dust is generated, and the population-averaged young age of  $\sim 20$  Myr would imply that this phase typically lasts  $\sim 40$  Myr. Alternatively, if all dark matter halos experience a single LAE phase shortly after their “formation” in a major merger, the mean halo occupation implies that LAEs will only be found in the youngest 1–10% of halos, which is barely consistent with their single-population best-fit age of 100 Myr. If LAEs represent a subset of dark matter halos selected to have ages less than 100 Myr, their observed clustering may underestimate their dark matter halo masses by up to a factor of two (see Gao & White 2007).

Figure 6 shows the reported bias values for LAEs to be lower than those of other  $z > 3$  galaxy populations (bias values determined as in Quadri et al. 2007). The expected evolution of bias is shown for the “no-merging” model (Fry 1996; White et al. 2007). A realistic amount of merging will cause the bias to drop somewhat faster, so the plotted trajectories provide an upper limit on the bias factor of a given point at lower redshifts. This shows that typical  $z = 3.1$  LAEs will evolve into galaxies of at most a few times  $L^*$  at  $z = 0$ . The bias values imply that LAEs at  $z = 3.1$  might evolve into the subset of BX galaxies at  $z \simeq 2.2$  dimmer than  $K = 21.5$ , which also show relatively weak clustering (Adelberger et al. 2005b). The  $K > 21.5$  BX galaxies have average  $M_* = 1.5 \times 10^{10} M_\odot$ , so the  $z = 3.1$  LAEs would need to form stars at an average rate of  $14 M_\odot \text{yr}^{-1}$  over the intervening Gyr. This could be achieved with a constant specific SFR and no merging or with a constant SFR and  $\sim 2$  major mergers. The only previous measurements of LAE clustering in unbiased fields are at  $z = 4.5$  (Kovač et al. 2007) and  $z = 4.86$  (Ouchi et al. 2003), and this earlier LAE population appears to have significantly stronger clustering, consistent with possibly evolving into typical Lyman break galaxies at  $z \simeq 3$ .

The models of Le Delliou et al. (2006) predict stellar and dark matter masses and star formation rates for  $z = 3$  LAEs within a factor of two of our results, despite assuming a top-heavy IMF and a very low escape fraction  $f_{esc} = 0.02$  that appears inconsistent with the observed lack of dust (see Kobayashi et al. 2007, for an alternative approach). Mao et al.

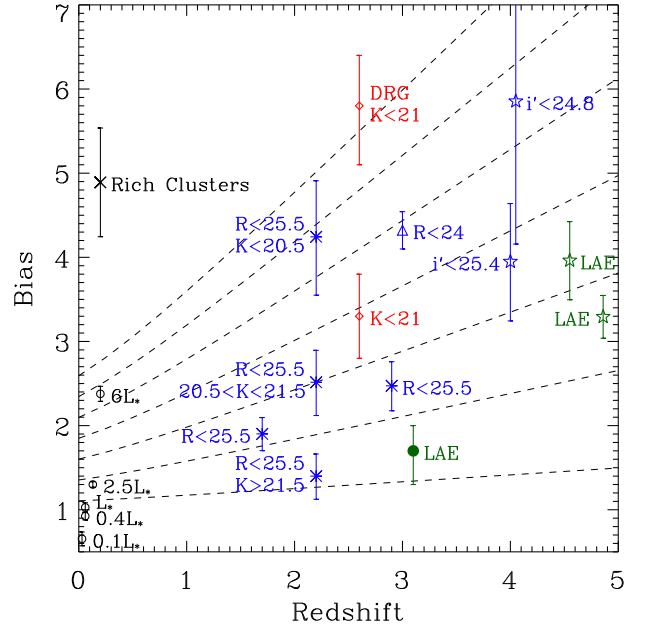


FIG. 6.— Tracks show the evolution of bias with redshift calculated using the no-merging model. The filled circle shows our result for the bias of LAEs at  $z = 3.1$ . Previous results at high-redshift are shown for LAEs at  $z = 4.5$  and  $z = 4.86$  (stars, Kovač et al. 2007 and Ouchi et al. 2003, respectively), LBGs at  $z \sim 4$  (stars, Ouchi et al. 2004), K-selected galaxies (diamonds, Quadri et al. 2007), bright LBGs at  $z \sim 3$  (triangle, Lee et al. 2006), and BM, BX, and LBG galaxies (asterisks, Adelberger et al. 2005a, Adelberger et al. 2005b). Local galaxy clustering is shown for SDSS galaxies (open circles, Zehavi et al. 2005) and for rich clusters (cross, Bahcall et al. 2003). K-band limits are in Vega magnitudes.

(2007) used the stellar mass of  $5 \times 10^8 M_\odot$  observed by Gawiser et al. (2006a) to predict LAE dark matter masses of  $10^{10} < M < 10^{11} M_\odot$ , in the lower end of our allowed range. The stellar ages of  $\sim 20$  Myr preferred by the two-population fit are noticeably lower than the maximum values of 100 to 500 Myr predicted by these authors, Mori & Umemura (2006), and Haiman & Spaans (1999), but the ages of 60 to 350 Myr preferred for the case of no evolved stars would be compatible.

None of the current models and numerical simulations of LAEs (see also Thommes & Meisenheimer 2005; Razoumov & Sommer-Larsen 2006; Tasitsiomi 2006) predict their present-day descendants. Nonetheless, the evolution of a significant fraction of  $z = 3.1$  LAEs into  $z = 0 L^*$  galaxies with dark matter mass  $M_{DM} \simeq 2 \times 10^{12} M_\odot$  and stellar mass  $M_* \simeq 4 \times 10^{10} M_\odot$  (Ichikawa et al. 2007) appears reasonable. Fig. 7 shows the histogram of present-day masses of dark matter halos in the Milli-Millennium merger trees that have progenitors with  $M > 5 \times 10^{10} M_\odot$  at  $z = 3.1$ . The median present-day halo mass is  $1.2 \times 10^{12} M_\odot$ , and this would increase if LAEs found in sub-halos of massive  $z = 3.1$  halos were included. Li et al. (2007) predict that the main progenitor of a present-day  $L^*$  galaxy had a dark matter mass of  $\sim 10^{11} M_\odot$  at  $z = 3$  and that these galaxies experienced several major mergers at  $1.5 < z < 7$ . To form an  $L^*$  galaxy at  $z = 0$ , several LAEs could merge while experiencing a mild reduction in average SFR, with accretion of lower-mass dark matter halos through minor mergers providing most of the final dark matter mass. However, the halo mass distribution of

$z = 0$  descendants in Fig.7 is very broad, with 25th and 75th percentile values of  $2.9 \times 10^{11} M_{\odot}$  and  $7.6 \times 10^{12} M_{\odot}$ . While  $z = 0$   $L^*$  galaxies like the Milky Way are roughly the median descendants of  $z = 3.1$  LAEs, the descendant halos include a wide range from dwarf galaxies to rich galaxy groups.

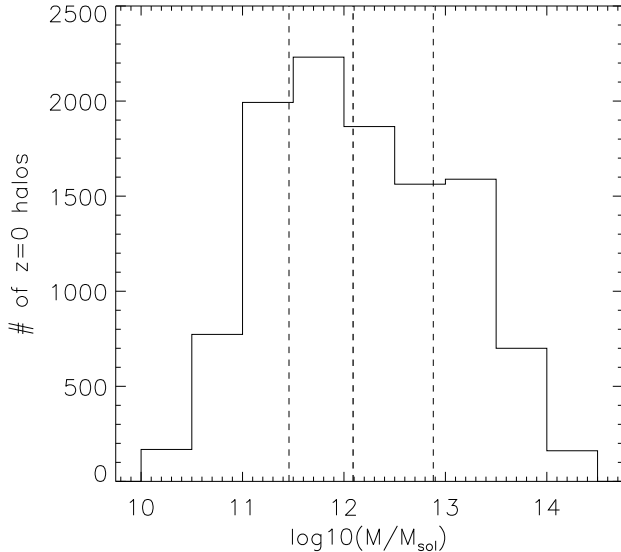


FIG. 7.— Histogram of dark matter halo masses of present-day descendants of halos with  $M > 5 \times 10^{10} M_{\odot}$  at  $z = 3.1$ . The dashed lines show the median halo mass of  $1.2 \times 10^{12} M_{\odot}$  and the 25th and 75th percentile values of  $2.9 \times 10^{11} M_{\odot}$  and  $7.6 \times 10^{12} M_{\odot}$ .

The typical LAE stellar mass at  $z = 3.1$  is lower than that of any other studied high-redshift population (see Reddy et al. 2006) but is close to that of dim ( $i < 26.3$ ) Lyman break galaxies (LBGs) at  $z \sim 5$  (Verma et al. 2007). LAEs at  $z = 3.1$  have much lower star formation rate, stellar age, stellar mass, dark matter halo mass, and dust extinction than the  $\sim 30 M_{\odot} \text{yr}^{-1}$ ,  $\sim 500$  Myr,  $\sim 2 \times 10^{10} M_{\odot}$ ,  $\sim 3 \times 10^{11} M_{\odot}$ ,  $A_V \simeq 1$  LBG population at  $z \sim 3$  ( $R < 25.5$ , Shapley et al. 2001; Adelberger et al. 2005b) or the  $\sim 100 M_{\odot} \text{yr}^{-1}$ ,  $\sim 2$  Gyr,  $\sim 10^{11} M_{\odot}$ ,  $\sim 10^{13} M_{\odot}$ ,  $A_V \simeq 2.5$  Distant Red Galaxy (DRG) population (Webb et al. 2006; Förster Schreiber et al. 2004; Quadri et al. 2007). The high-redshift Sub-Millimeter Galaxies (Chapman et al. 2003) appear to be the most massive and dusty, with the highest SFR. LAEs may represent the beginning of an evolutionary sequence where galaxies gradually become more massive and dusty due to mergers and star formation, but most LAEs at  $z = 3.1$  will never reach the DRG stage since DRG stellar and

dark matter masses are already greater than those of present-day  $L^*$  galaxies.

The Damped Ly $\alpha$  Absorption systems (DLAs, Wolfe et al. 2005) are another high-redshift population that probes the faint end of the luminosity function. The dark matter halo masses of DLAs at  $z \sim 3$  were determined by Cooke et al. (2006) to lie in the range  $10^9 < M < 10^{12} M_{\odot}$  i.e.,  $1.3 < b < 4$ , which overlaps with the range of both  $L^*$  and super- $L^*$  progenitors in Fig. 6. At least half of the DLAs appear to have ongoing star formation (Wolfe et al. 2004) and two of the three DLAs detected in emission were seen in Ly $\alpha$ . Further study is needed to determine the relationship between DLAs and LAEs.

The observed properties of LAEs at  $z = 3.1$  make them the most promising candidates to be high-redshift progenitors of present-day  $L^*$  galaxies like the Milky Way. Our results suggest that LAEs are observed during the early phases of a burst of star formation, perhaps caused by a major merger of smaller dark matter halos. The input halos appear to have already contained stars, accounting for the evolved stellar population that appears to contribute most of the LAE stellar mass, although starburst-only models are also allowed. It is clear that not all progenitors of  $L^*$  galaxies were LAEs at  $z = 3.1$ . The comoving number density of our sample of LAEs is a factor of 15 less than  $\phi^*$  for local galaxies (Lin et al. 1996), plus we expect several high-redshift halos to merge into a single galaxy today. It remains possible that all progenitors of present-day galaxies experienced an LAE phase at *some* redshift. Clustering and SED studies of LAEs at various redshifts are needed to assess the validity of this hypothesis.

We acknowledge valuable conversations with Kyoung-Soo Lee, Jeff Newman, Ravi Sheth, David Spergel, Jason Tumlinson and Martin White. We are grateful for support from Fundación Andes, the FONDAF Centro de Astrofísica, and the Yale Astronomy Department. Support for this work was provided by NASA through an award issued by JPL/Caltech. This material is based upon work supported by the National Science Foundation under Grant Nos. AST-0201667, an NSF Astronomy and Astrophysics Postdoctoral Fellowship (AAPF) awarded to E.G., and AST-0137927 awarded to R.C. We thank the staff of Cerro Tololo Inter-American Observatory and Las Campanas Observatory for their invaluable assistance with our observations. The Millenium Simulation databases used in this paper and the web application providing online access to them were constructed as part of the activities of the German Astrophysical Virtual Observatory. This research has made use of NASA's Astrophysics Data System. Facilities:CTIO(MOSAIC II),LCO(IMACS)

#### REFERENCES

- Adelberger, K. L., Erb, D. K., Steidel, C. C., Reddy, N. A., Pettini, M., & Shapley, A. E. 2005a, ApJ, 620, L75  
 Adelberger, K. L., Steidel, C. C., Pettini, M., Shapley, A. E., Reddy, N. A., & Erb, D. K. 2005b, ApJ, 619, 697  
 Alexander, D. M. et al. 2003, AJ, 126, 539  
 Arnaboldi, M., Aguerri, J. A. L., Napolitano, N. R., Gerhard, O., Freeman, K. C., Feldmeier, J., Capaccioli, M., Kudritzki, R. P., & Méndez, R. H. 2002, AJ, 123, 760  
 Bahcall, N. A., Dong, F., Hao, L., Bode, P., Annis, J., Gunn, J. E., & Schneider, D. P. 2003, ApJ, 599, 814  
 Calzetti, D., Armus, L., Bohlin, R. C., Kinney, A. L., Koornneef, J., & Storchi-Bergmann, T. 2000, ApJ, 533, 682  
 Castro Cerón, J. M., Michałowski, M. J., Hjorth, J., Watson, D., Fynbo, J. P. U., & Gorosabel, J. 2006, ApJ, 653, L85  
 Chapman, S. C., Windhorst, R., Odewahn, S., Yan, H., & Conselice, C. 2003, ApJ, 599, 92  
 Cooke, J., Wolfe, A. M., Gawiser, E., & Prochaska, J. X. 2006, ApJ, 652, 994  
 Cowie, L. L. & Hu, E. M. 1998, AJ, 115, 1319  
 Dawson, S. et al. 2004, ApJ, 617, 707  
 Dickinson, M., Giavalisco, M., & The Goods Team. 2003, in The Mass of Galaxies at Low and High Redshift, 324  
 Fazio, G. G. et al. 2004, ApJS, 154, 10  
 Finkelstein, S. L., Rhoads, J. E., Malhotra, S., Pirzkal, N., & Wang, J. 2007, ApJ, 660, 1023

- Förster Schreiber, N. M. et al. 2004, *ApJ*, 616, 40
- Fry, J. N. 1996, *ApJ*, 461, L65
- Gao, L. & White, S. D. M. 2007, *MNRAS*, 377, L5
- Gawiser, E. et al. 2006a, *ApJ*, 642, L13
- 2006b, *ApJS*, 162, 1
- Gronwall, C. et al. 2007, *ApJ*, 667, 79
- Haiman, Z. & Spaans, M. 1999, *ApJ*, 518, 138
- Hansen, M. & Oh, S. P. 2006, *MNRAS*, 367, 979
- Hogg, D. W., Cohen, J. G., Blandford, R., & Pahre, M. A. 1998, *ApJ*, 504, 622
- Hu, E. M., Cowie, L. L., Capak, P., McMahon, R. G., Hayashino, T., & Komiyama, Y. 2004, *AJ*, 127, 563
- Hu, E. M., Cowie, L. L., & McMahon, R. G. 1998, *ApJ*, 502, L99
- Hu, E. M. & McMahon, R. G. 1996, *Nature*, 382, 231
- Ichikawa, T. et al. 2007, *ArXiv:astro-ph/0701820*
- Infante, L. 1994, *A&A*, 282, 353
- Kobayashi, M. A. R., Totani, T., & Nagashima, M. 2007, *ApJ*, in press, arXiv:0705.4349
- Kovač, K., Somerville, R. S., Rhoads, J. E., Malhotra, S., & Wang, J. 2007, *ApJ*, 668, 15
- Kudritzki, R.-P. et al. 2000, *ApJ*, 536, 19
- Lai, K., Huang, J.-S., Fazio, G., Cowie, L. L., Hu, E. M., & Kakazu, Y. 2007a, *ApJ*, 655, 704
- Lai, K. et al. 2007b, *ApJ*, submitted
- Landy, S. D. & Szalay, A. S. 1993, *ApJ*, 412, 64
- Le Delliou, M., Lacey, C. G., Baugh, C. M., & Morris, S. L. 2006, *MNRAS*, 365, 712
- Lee, K.-S., Giavalisco, M., Gnedin, O. Y., Somerville, R. S., Ferguson, H. C., Dickinson, M., & Ouchi, M. 2006, *ApJ*, 642, 63
- Lehmer, B. D. et al. 2005, *ApJS*, 161, 21
- Li, Y., Mo, H. J., van den Bosch, F. C., & Lin, W. P. 2007, *MNRAS*, 379, 689
- Lin, H., Kirshner, R. P., Sheth, S. A., Landy, S. D., Oemler, A., Tucker, D. L., & Schechter, P. L. 1996, *ApJ*, 471, 617
- Manning, C., Stern, D., Spinrad, H., & Bunker, A. J. 2000, *ApJ*, 537, 65
- Mao, J., Lapi, A., Granato, G. L., de Zotti, G., & Danese, L. 2007, *ApJ*, 667, 655
- Maraston, C. 2005, *MNRAS*, 362, 799
- Matsuda, Y., Yamada, T., Hayashino, T., Yamauchi, R., & Nakamura, Y. 2006, *ApJ*, 640, L123
- Mori, M. & Umemura, M. 2006, *Nature*, 440, 644
- Neufeld, D. A. 1991, *ApJ*, 370, L85
- Nilsson, K. K., Moeller, P., Moeller, O., Fynbo, J. P. U., Michalowski, M. J., Watson, D., Ledoux, C., Rosati, P., Pedersen, K., & Grove, L. F. 2007, *A&A*, 471, 71
- Ouchi, M. et al. 2003, *ApJ*, 582, 60
- 2004, *ApJ*, 611, 685
- Peebles, P. J. E. 1980, *The Large-Scale Structure of the Universe* (Princeton, NJ: Princeton University Press)
- Pirzkal, N., Malhotra, S., Rhoads, J. E., & Xu, C. 2007, *ApJ*, 667, 49
- Quadri, R. et al. 2007, *ApJ*, 654, 138
- Razoumov, A. O. & Sommer-Larsen, J. 2006, *ApJ*, 651, L89
- Reddy, N. A., Steidel, C. C., Erb, D. K., Shapley, A. E., & Pettini, M. 2006, *ApJ*, 653, 1004
- Rhoads, J. E. et al. 2003, *AJ*, 125, 1006
- Salpeter, E. E. 1955, *ApJ*, 121, 161
- Shapley, A. E., Steidel, C. C., Adelberger, K. L., Dickinson, M., Giavalisco, M., & Pettini, M. 2001, *ApJ*, 562, 95
- Sheth, R. K. & Tormen, G. 1999, *MNRAS*, 308, 119
- Simon, P. 2007, *A&A*, 473, 711
- Somerville, R. S., Lee, K., Ferguson, H. C., Gardner, J. P., Moustakas, L. A., & Giavalisco, M. 2004, *ApJ*, 600, L171
- Spergel, D. N. et al. 2007, *ApJS*, 170, 377
- Springel, V. et al. 2005, *Nature*, 435, 629
- Stern, D., Bunker, A., Spinrad, H., & Dey, A. 2000, *ApJ*, 537, 73
- Tasitsiomi, A. 2006, *ApJ*, 645, 792
- Terlevich, R., Melnick, J., Masegosa, J., Moles, M., & Copetti, M. V. F. 1991, *A&AS*, 91, 285
- Thommes, E. & Meisenheimer, K. 2005, *A&A*, 430, 877
- Venemans, B. P. et al. 2005, *A&A*, 431, 793
- Verma, A., Lehnert, M. D., Förster Schreiber, N. M., Bremer, M. N., & Douglas, L. 2007, *MNRAS*, 377, 1024
- Virani, S. N., Treister, E., Urry, C. M., & Gawiser, E. 2006, *AJ*, 131, 2373
- Webb, T. M. et al. 2003, *ApJ*, 582, 6
- Webb, T. M. A. et al. 2006, *ApJ*, 636, L17
- White, M., Zheng, Z., Brown, M. J. I., Dey, A., & Jannuzi, B. T. 2007, *ApJ*, 655, L69
- Wolfe, A. M., Gawiser, E., & Prochaska, J. X. 2005, *ARA&A*, 43, 861
- Wolfe, A. M., Howk, J. C., Gawiser, E., Prochaska, J. X., & Lopez, S. 2004, *ApJ*, 615, 625
- Zehavi, I. et al. 2005, *ApJ*, 630, 1
- Zheng, Z., Coil, A. L., & Zehavi, I. 2007, *ApJ*, 667, 760